Journal of Experimental Botany, Vol. 71, No. 2 pp. 730–741, 2020
doi:10.1093/jxb/erz376 Advance Access Publication September 26, 2019
This paper is available online free of all access charges (see https://academic.oup.com/jxb/pages/openaccess for further details)

RESEARCH PAPER

Glutathione redox state plays a key role in flower development and pollen vigour

Estefanía García-Quirós[1,2], Juan de Dios Alché[1], Barbara Karpinska[3], and Christine H. Foyer[2,3,*]

[1] Plant Reproductive Biology and Advanced Microscopy Laboratory, Department of Biochemistry, Cell and Molecular Biology of Plants, Estación Experimental del Zaidín, CSIC, 18008 Granada, Spain
[2] Centre for Plant Sciences, School of Biology, Faculty of Biological Sciences, University of Leeds, Leeds LS2 9JT, UK
[3] School of Biosciences, College of Life and Environmental Sciences, University of Birmingham, Birmingham B15 2TT, UK

* Correspondence: c.h.foyer@bham.ac.uk

Received 2 May 2019; Editorial decision 6 August 2019; Accepted 10 August 2019

Editor: Zoe Wilson, University of Nottingham, UK

Abstract

The importance of the glutathione pool in the development of reproductive tissues and in pollen tube growth was investigated in wild-type (WT) *Arabidopsis thaliana*, a reporter line expressing redox-sensitive green fluorescent protein (roGFP2), and a glutathione-deficient *cad2-1* mutant (*cad2*-1/roGFP2). The *cad2*-1/roGFP2 flowers had significantly less reduced glutathione (GSH) and more glutathione disulfide (GSSG) than WT or roGFP2 flowers. The stigma, style, anther, germinated pollen grains, and pollen tubes of roGFP2 flowers had a low degree of oxidation. However, these tissues were more oxidized in *cad2*-1/roGFP2 flowers than the roGFP2 controls. The ungerminated pollen grains were significantly more oxidized than the germinated pollen grains, indicating that the pollen cells become reduced upon the transition from the quiescent to the metabolically active state during germination. The germination percentage was lower in *cad2-1*/roGFP2 pollen and pollen tube growth arrested earlier than in roGFP2 pollen, demonstrating that increased cellular reduction is essential for pollen tube growth. These findings establish that ungerminated pollen grains exist in a relatively oxidized state compared with germinating pollen grains. Moreover, failure to accumulate glutathione and maintain a high GSH/GSSG ratio has a strong negative effect on pollen germination.

Keywords: Flower development, glutathione, oxidative stress, pollen germination, redox regulation, redox-sensitive green fluorescent protein (roGFP).

Introduction

The tripeptide thiol γ-glutamylcysteine glycine (glutathione, GSH) is the most abundant low-molecular-weight thiol in plants and animals (Noctor *et al.*, 2011). GSH synthesis in the cytosol and plastids of plant cells (Wachter *et al.*, 2005; Galant *et al.*, 2011) occurs via the sequential action of two ATP-dependent enzymes, γ-glutamylcysteine synthetase (γ-ECS), also called γ-glutamylcysteine ligase, and glutathione synthase (GS) (Cairns *et al.*, 2006; Pasternak *et al.*, 2008; Galant *et al.*, 2011; Noctor *et al.*, 2011). In the first step, γ-glutamylcysteine (γ-EC) is produced from cysteine and glutamate by the action of γ-ECS. In the second step, glycine is added to γ-EC to form GSH by the action of GS (Noctor *et al.*, 2002; Sugiyama *et al.*, 2004; Wachter *et al.*, 2005; Galant *et al.*, 2011). GSH synthesis is regulated by the availability of cysteine or glycine and by the post-translational redox activation of γ-ECS via the formation of an intramolecular disulfide bond (Cys186-Cys406 in Arabidopsis) (Noctor, *et al.*, 2002; Gromes, *et al.*, 2008). In this way GSH synthesis is regulated by the redox

environment of the chloroplast, allowing rapid responses to biotic and abiotic stresses.

Knockout γ-ECS mutants are lethal (Cairns *et al.*, 2006). However, there are a number of Arabidopsis mutants with defects in γ-ECS that allow a lower level of GSH synthesis (Cobbett *et al.*, 1998; Ball *et al.*, 2004). These mutants have significantly lower levels of GSH accumulation than the wild type (WT), and have no marked shoot phenotypes but variable effects on root system development and architecture (Schnaubelt *et al.*, 2013). For example, very low levels of GSH are present in the *rml1* mutant, leading to arrest of the root apical meristem (Vernoux *et al.*, 2000; Schnaubelt *et al.*, 2013). In contrast, the *cad2-1* mutant contains ~30% of WT GSH levels and shows some effects on lateral root production (Schnaubelt *et al.*, 2013).

GSH and γ-EC are exported from the chloroplasts to the cytosol by CLT transporters, but the mechanisms of import of GSH into mitochondria and other cellular compartments are largely unknown (Gigolashvili and Kopriva, 2014; Zechmann, 2014). GSH accumulates at high concentrations (5–10 mM) in plant cells and is directly involved in the maintenance of intracellular redox homeostasis, acting as a redox buffer (Meister *et al.*, 1983; Schafer *et al.*, 2001; López-Mirabal *et al.*, 2008; Noctor *et al.*, 2011, 2016). Like ascorbate, GSH serves to limit the accumulation of reactive oxygen species (ROS) within plant cells (Mittler *et al.*, 2004; Foyer and Noctor, 2005, 2009, 2011; Noctor *et al.*, 2012; Mittler, 2017). As a result of interactions with ROS, GSH is oxidized to glutathione disulfide (GSSG). GSSG is reduced back to GSH by the action of glutathione reductase (Schwarzländer *et al.*, 2008; Marty *et al.*, 2009; García-Quirós *et al.*, 2017). GSH and GSSG are key players in cellular redox regulation, governing the redox potential and ensuring a stable redox environment within the cell. GSH and GSSG are also involved in the control of gene expression (Foyer *et al.*, 2001; Maughan and Foyer, 2006). However, *in vivo* measurements of the glutathione pool have revealed that the cytosol, nuclei, and mitochondria contain very little GSSG, and that oxidative challenges are rapidly counterbalanced by the network of other antioxidants (Queval *et al.*, 2009; Noctor *et al.*, 2011, 2016; de Simone *et al.*, 2017). Moreover, GSSG can be rapidly sequestered in the vacuole (Noctor *et al.*, 2013).

Together with nitric oxide (Airaki *et al.*, 2011), ROS and GSH are key regulators of plant development (Considine and Foyer, 2014). These redox molecules are particularly important in the development of flowers and in pollen germination (Zechmann and Müller, 2010; Zechmann *et al.*, 2011*a*, *b*; Traverso *et al.*, 2013; Schippers *et al.*, 2016). GSH functions together with NADPH-thioredoxin (TRX)-reductase NTR/TRX pathways to regulate auxin signalling during and after pollen germination (Zechmann *et al.*, 2011*a, b*; Traverso *et al.*, 2013). GSH depletion triggers alterations in auxin metabolism that lead to the inhibition of pollen germination. This observation is likely to be linked to changes in ROS accumulation that occur in the reproductive tissues during pollen and pistil development, pollen tube germination, and pollen–pistil interactions (Zafra *et al.*, 2010). However, the relevance of glutathione-dependent pathways remains poorly understood, and too little is known about the compartment-specific changes in redox processes that occur during flower and pollen development.

A combination of different techniques has been used to investigate the role of glutathione in fertilization and the germination of the pollen tube. Specific antibodies were used to characterize the abundance of GSH in flowers during development. In addition, the effects of low GSH in the cytosol and nuclei of *Arabidopsis thaliana* reproductive tissues were determined using *in vivo* redox-sensitive green fluorescent protein (roGFP) reporter lines (Meyer *et al.*, 2007). roGFP-expressing WT (roGFP2) and *cad2-1* mutant (*cad2*-1/roGFP2) reporter lines were used in the present study to estimate the redox state of the nuclei and cytosol of flower and pollen cells to provide some of the missing pieces of information required to decipher the role of glutathione in these key processes.

Materials and methods

Plant material and growth conditions

Seeds of WT *Arabidopsis thaliana* accession Columbia-0 (Col-0), Col-0 expressing roGFP2 (de Simone *et al.*, 2017), and *cad2-1* mutants expressing roGFP2 (*cad2-1*/roGFP2) were surface sterilized and washed twice with sterile water. After stratification for 2 days in the dark at 4 °C, seeds were sown on soil and grown in controlled environment chambers under 120–150 μmol m^{-2} s^{-1} irradiance with an 8 h/16 h day/night period, 22 °C/18 °C day/night temperatures, and a relative humidity of 60%. Samples were collected from 6-week-old plants bearing flowers at different stages (Alvarez-Buylla *et al.*, 2010). Samples were collected from younger flower buds at flowering stage 6–7, with sepals that still enclose buds and anthers (at meiosis) and tetrads. Flowers were also collected from later stages of flowering, particularly flowering stage 11–12 (when petals, stamens and pollen at the bicellular–tricellular transition are present), flowering stage 13 (when stamens outstrip the gynoecium and anthers dehisce), and flowering stage 14 (when dehiscent anthers extend above the stigma). Each experiment was repeated three times and results are the average of three independent experiments.

Pollen germination

A total of 25–30 freshly opened flowers (at stage 14) of Arabidopsis were collected and allowed to dry at room temperature for 30 min in a 1.5 ml tube with the lid opened. A 1 ml volume of germination medium (Fan *et al.*, 2001) was added and the pollen was concentrated according to Li (2011). The pollen grains were germinated at 28 °C and in the dark for 1, 2, and 3 h. Images of germinated pollen grains were taken in a Leica DMI600B or a Nikon Eclipse TE2000-U inverted epifluorescence microscope. The germination of the pollen was assessed by counting the germinated grains (those in which the pollen tube length was greater than the pollen diameter) at the different germination times, and expressing the number of germinated grains as a percentage of the total number of pollen grains. The length of the pollen tubes was calculated using the Straight tool of ImageJ software. Data presented are the means and SD of a minimum of nine different samples of each one of three experimental replicates.

Sample preparation for immunohistochemistry

Samples were collected at the different developmental stages identified in the figure legends and immersed in a fixative solution (4% paraformaldehyde and 0.2% glutaraldehyde in 0.05 M sodium cacodylate buffer, pH 7.2). Further dehydration in an ethanol series and embedding in Unicryl resin followed by polymerization using UV light at –20 °C were performed. Thin sections (1 μm) were attached to 3-triethoxysilylpropylamine-treated slides.

Immunolabelling of glutathione

Thin sections were incubated in phosphate-buffered saline (pH 7.2) containing 2.5% bovine serum albumin (Sigma-Aldrich) for 1 h at room

temperature and then treated with primary anti-GSH antibody (Agrisera prod. No. AS09 594) followed by secondary antibody (anti-rabbit IgG Alexa549-labelled secondary antibody; Molecular Probes). Negative controls were prepared by omitting the primary antibody. After washing three times, samples were mounted with citifluor (Ted Pella). Fluorescence microscopy observations were performed using a Nikon Eclipse TE2000-U inverted microscope fitted with a ProgRes MF Cool CCD microscope camera (Jenoptik). Fluorescence intensity was quantified using ImageJ software. Data presented are the average of a minimum of nine images obtained in three independent experiments.

Liquid chromatography–electrospray/mass spectrometry

Tissue glutathione contents were determined by liquid chromatography–electrospray/mass spectrometry (LC-ES/MS). Samples of open flowers and floral buds (green and white) of WT, roGFP2, and *cad*2-1/roGFP2 plants were frozen in liquid nitrogen, ground, and immediately homogenized in 1 ml 0.1 M HCl. After centrifugation, supernatants were extracted again. The supernatants were pooled and filtered through 0.45 mm polyvinylidene fluoride filters and analysed by LC-ES/MS on a Triple quadrupole mass spectrometer (Quattro micro) coupled to a liquid chromatograph (Waters Alliance 2695) with dual wavelength detector.

Confocal laser scanning microscopy and image analysis

Freshly opened flowers (day 0 according to Boavida *et al.*, 2007) were incubated in 1 ml of germination medium (Fan *et al.*, 2001) at 28 °C for 1 h in darkness. After the incubation, selected flowers were assembled on excavated slides containing a few drops of the germination medium. They were immediately observed with a C-1 confocal microscope (Nikon) fitted on a Nikon Eclipse TE2000-U inverted microscope, using an image capture schedule equivalent to that described by de Simone *et al.* (2017). Briefly, the image of reduced roGFP (green) was calculated by subtracting the image after excitation with 405 nm from the image obtained after excitation with 488 nm, by using ImageJ software. The final reduced roGFP/oxidized roGFP ratios were also determined with ImageJ, by using a threshold of 10. Finally, to better illustrate the redox potential differences in the images evaluated, the grayscale was converted to a false-colour scale image using the ImageJ 'Fire' query table. All measurements were taken with identical adjustments to be able to compare them in absolute terms (Meyer *et al.*, 2007). The intensity per area was measured in each image by using ImageJ software, and these data were used to determine the degree of oxidation and the redox potential in each tissue examined according to the Nernst equation (de Simone *et al.*, 2017). A minimum of 10 samples per treatment were analysed.

Statistical analysis

IBM SPSS Statistics software (version 21.0.0.0) was used to analyse the statistical significance of the results. The Shapiro–Wilk test combined with the Kolmogorov–Smirnov test was used to evaluate the normality of the data. A one-way ANOVA was performed in combination with a Duncan's multiple range test and *post hoc* Bonferroni procedure to verify the statistical significance of the data.

Results

Immunolocalization of GSH during flower development

GSH was detected in the microsporocytes, tetrads, pollen grains, and anther tissues (including the tapetum) of the WT, roGFP2, and cad2-1/roGFP2 plants using anti-GSH antibody (Figs 1–3). GSH was also present in the gynoecium (including stigma), the embryo sacs, and other tissues of the ovary (Figs 4–6) of the WT and roGFP2 plants.

GSH was present in the nuclei, cytosol, apoplast/cell wall compartment, tapetum, and embryo sacs of these lines. GSH and GSSG are transported throughout the plant, and both metabolites are readily taken up by the plasma membrane. Low levels of GSH and GSSG have been detected in the apoplastic fluid of leaf cells (Vanacker *et al.*, 1998), consistent with our findings. The antibody-linked fluorescence was much less intense in all the flower tissues of the *cad2*-1/roGFP2 plants than either the WT or roGFP2 plants. This observation reflects the lower levels of GSH present in the *cad2*-1/roGFP2 plants than the other lines, which had similar levels of GSH during all developmental stages, especially at the end of anther development (Fig. 7).

LC-ES/MS determination of GSH and GSSG levels

The levels of GSH and GSSG were similar in WT (Fig. 8A) and roGFP2 (Fig. 8B) flowers at all stages of development. The highest levels of GSH were determined in flowers at stage 14, with high GSH/GSSG ratios maintained throughout flower development in the WT (Fig. 8A) and roGFP2 (Fig. 8B) plants. In contrast, the flowers of *cad2*-1/roGFP2 plants had less than 50% of the GSH present in WT or roGFP2 lines at equivalent stages of flower development. Moreover, the levels of GSSG in *cad2*-1/roGFP2 flowers (Fig. 8C) were similar to or slightly higher than those detected in WT (Fig. 8A) and roGFP2 (Fig. 8B) flowers, resulting in lower GSH/GSSG ratios.

Redox state of the glutathione pool in vivo

roGFP fluorescence was readily detected in the anthers, pistils, and germinated pollen grains of roGFP2 and *cad2*-1/roGFP2 plants (Figs 9–11). The degree of oxidation was low in the stigma, style, anther, germinated pollen grains, and pollen tubes of roGFP2 flowers (Fig. 12), suggesting that the glutathione pool is highly reduced in these tissues. This finding is in agreement with the data obtained by biochemical analysis of the tissues described above. In contrast, the ungerminated pollen grains were significantly more oxidized than the germinated pollen grains (Fig. 12). The degree of oxidation was also higher in the ungerminated pollen grains of *cad2-1*/roGPF2 flowers compared with germinated pollen grains and other tissues (Fig. 12). All tissues (stigma, style, anther, mature and germinated pollen grains, and pollen tubes) of the *cad2*-1/roGFP2 flowers tended to be more oxidized than the respective tissues of roGFP2 flowers (Fig. 12). However, these differences were statistically significant only for stigma, anther, and mature pollen.

The glutathione redox potentials were similar in the stigma, style, anther, germinated pollen grains, and pollen tubes of the roGFP2 flowers (Fig. 13). However, the glutathione redox potential of the ungerminated pollen grains was significantly lower than that of the germinated pollen grains of roGFP2 (Fig. 13). The degree of oxidation was lower in the stigma, style, anther, germinated pollen grains, and pollen tubes of *cad2*-1/roGFP2 flowers than in roGFP2 plants (Fig. 13). The most positive glutathione redox potentials were determined in the ungerminated pollen grains. These values were significantly more positive than those calculated for the roGFP2 plants (Fig. 13).

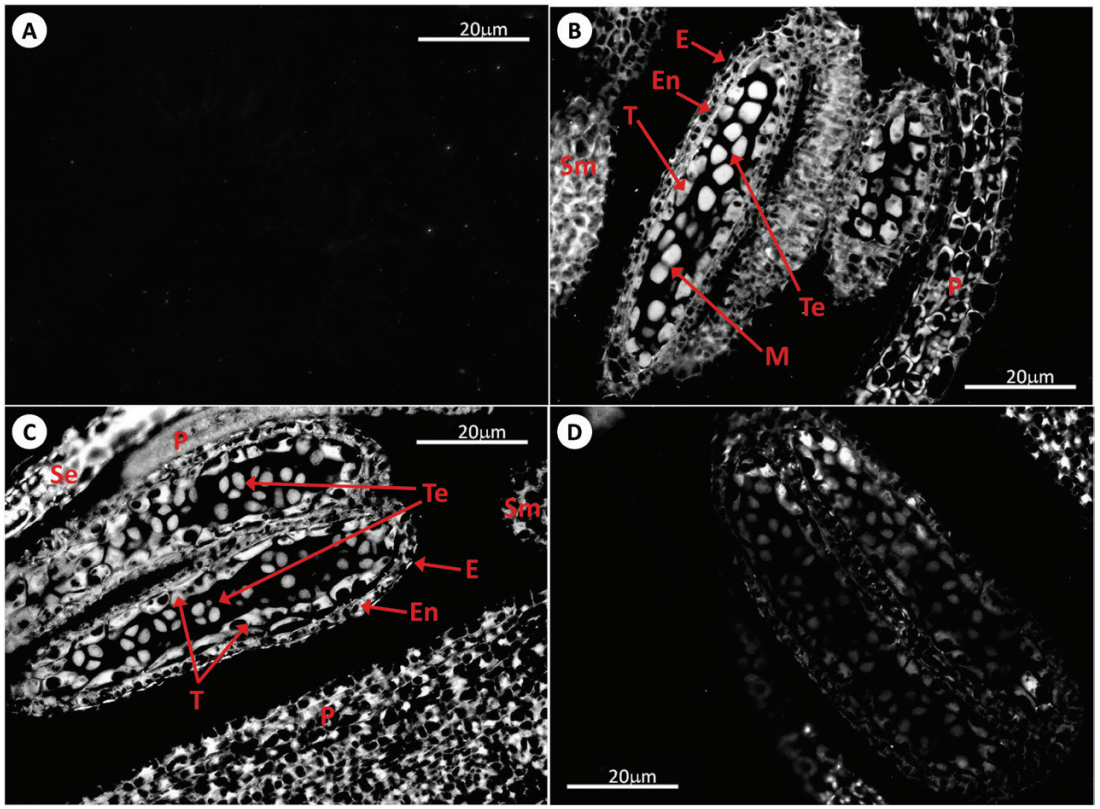

Fig. 1. Immunolocalization of GSH by antibody-associated fluorescence microscopy in Arabidopsis anthers at stages 6–7 of development. (A) Negative control (meiocytes); (B) WT (meiocytes); (C) roGFP2 (tetrads); (D) *cad2*-1/roGFP2 (meiocytes). E, epidermis; En, endothecium; M, meiosis; P, petal; Se, sepal; Sm, stamen; T, tapetal layer; Te, tetrad.

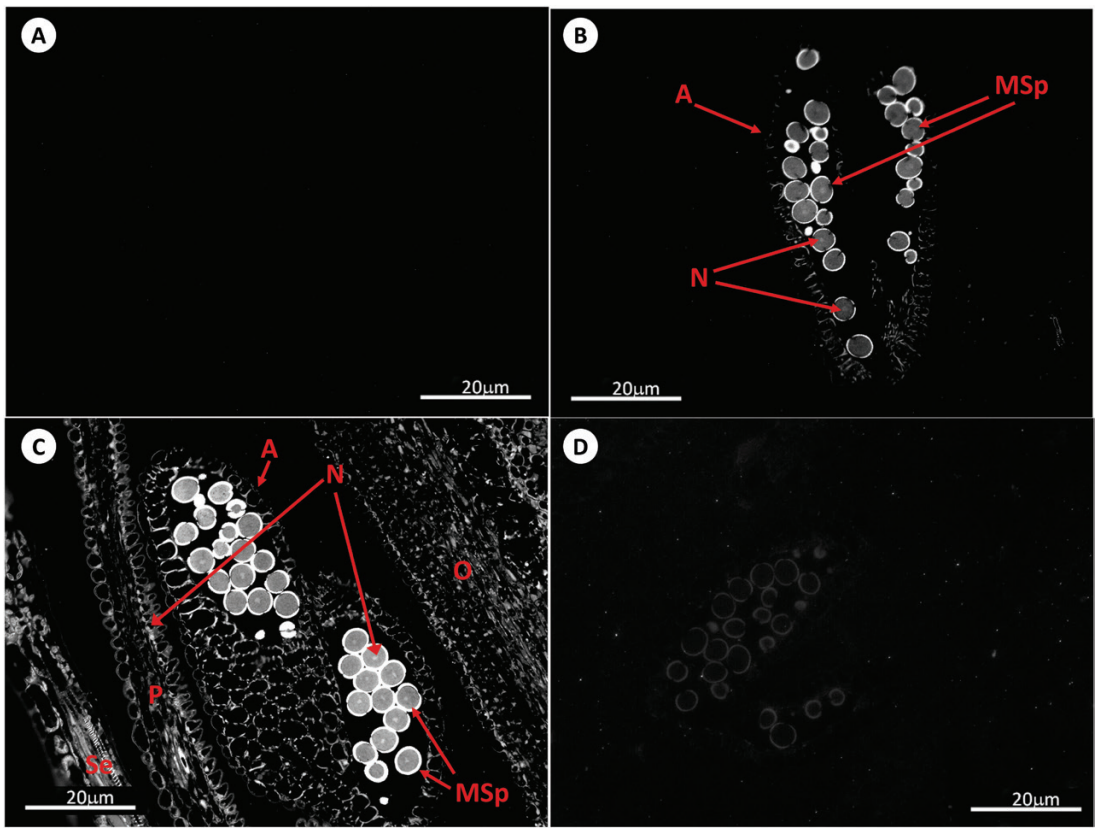

Fig. 2. Immunolocalization of GSH by antibody-associated fluorescence microscopy in Arabidopsis anthers at stage 13. (A) Negative control; (B) WT; (C) roGFP2; (D) *cad2*-1/roGFP2. A, anther; MSp, microspores; N, nucleus; O, ovary; P, petal; Se, sepal.

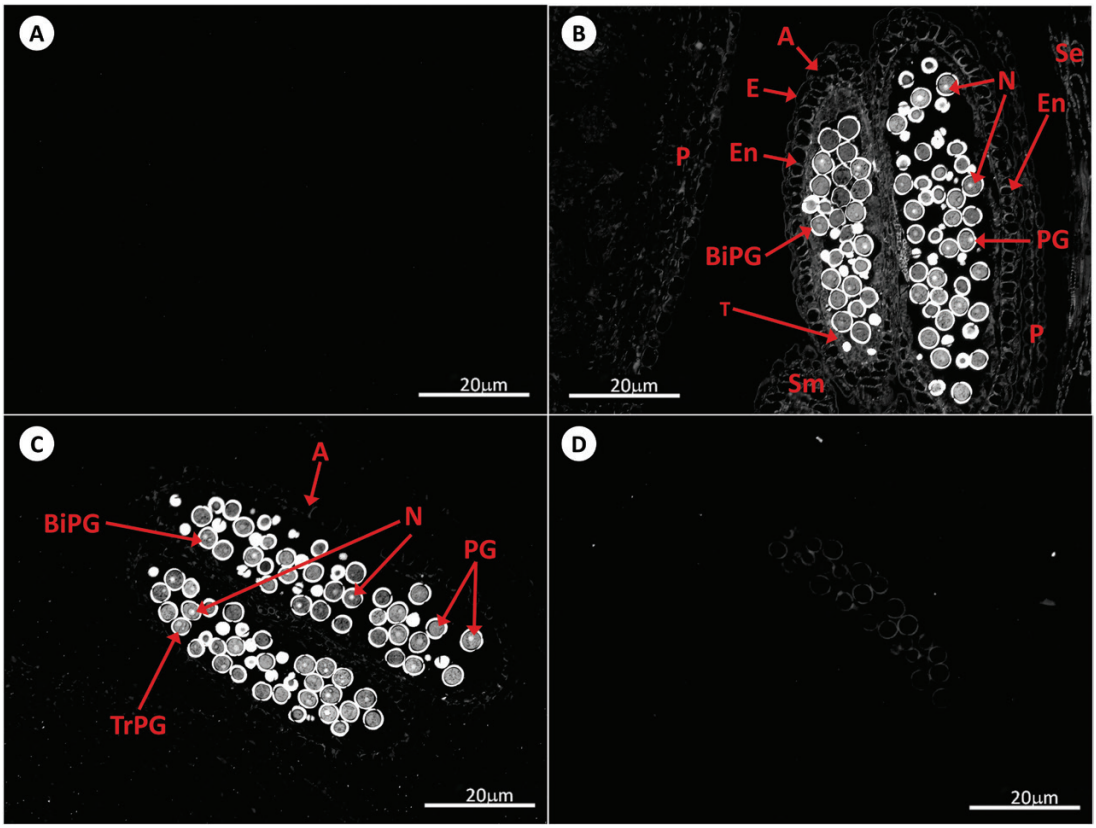

Fig. 3. Immunolocalization of GSH by antibody-associated fluorescence microscopy in Arabidopsis anthers at stage 14. (A) Negative control; (B) WT; (C) roGFP2; (D) *cad2*-1/roGFP2. A, anther; BiPG, bicellular pollen grain; E, epidermis; En, endothecium; N, nucleus; P, petal; PG, pollen grain; Se, sepal; Sm, stamen; T, tapetal layer; TrPG, tricellular pollen grain.

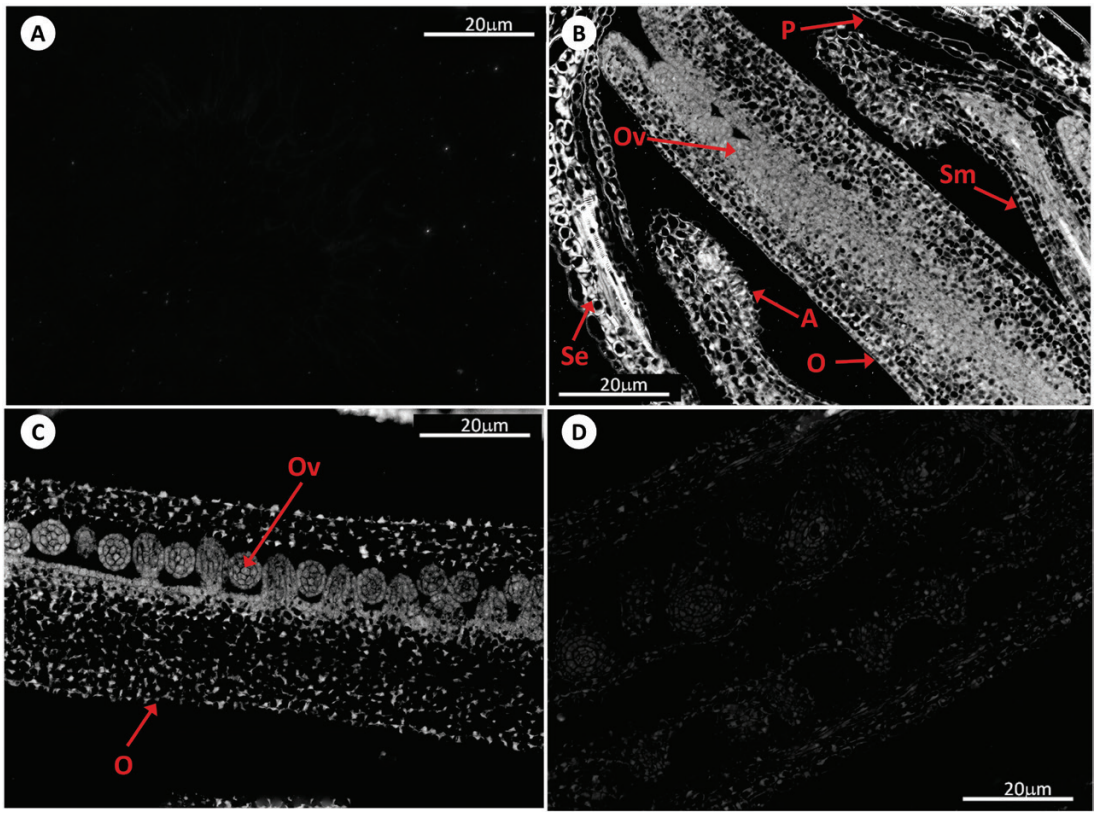

Fig. 4. Immunolocalization of GSH by antibody-associated fluorescence microscopy in Arabidopsis flowers (pistils) at stage 11–12. (A) Negative control; (B) WT; (C) roGFP2; (D) *cad2*-1/roGFP2. A, anther; O, ovary; Ov, ovum; P, petal; Se, sepal; Sm, stamen.

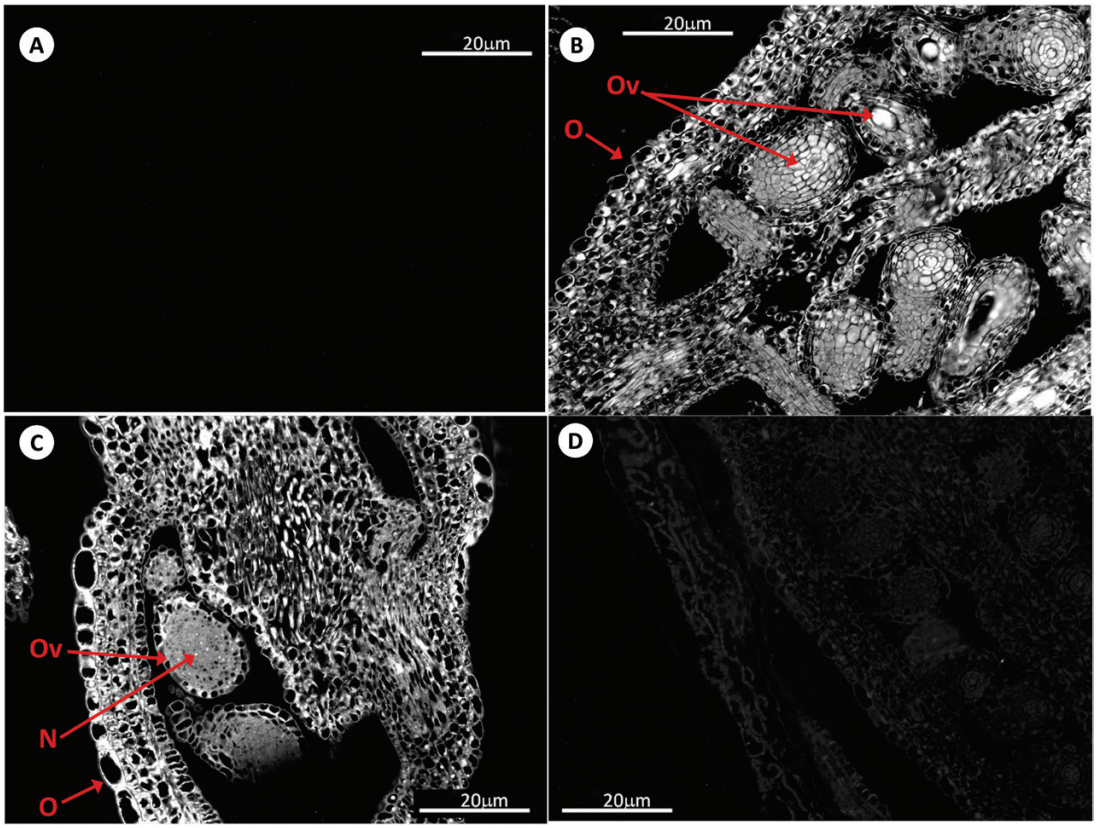

Fig. 5. Immunolocalization of GSH by antibody-associated fluorescence microscopy in Arabidopsis pistils at stage 13. (A) Negative control; (B) WT; (C) roGFP2; (D) *cad2*-1/roGFP2. N, nucleus; O, ovary; Ov, ovum.

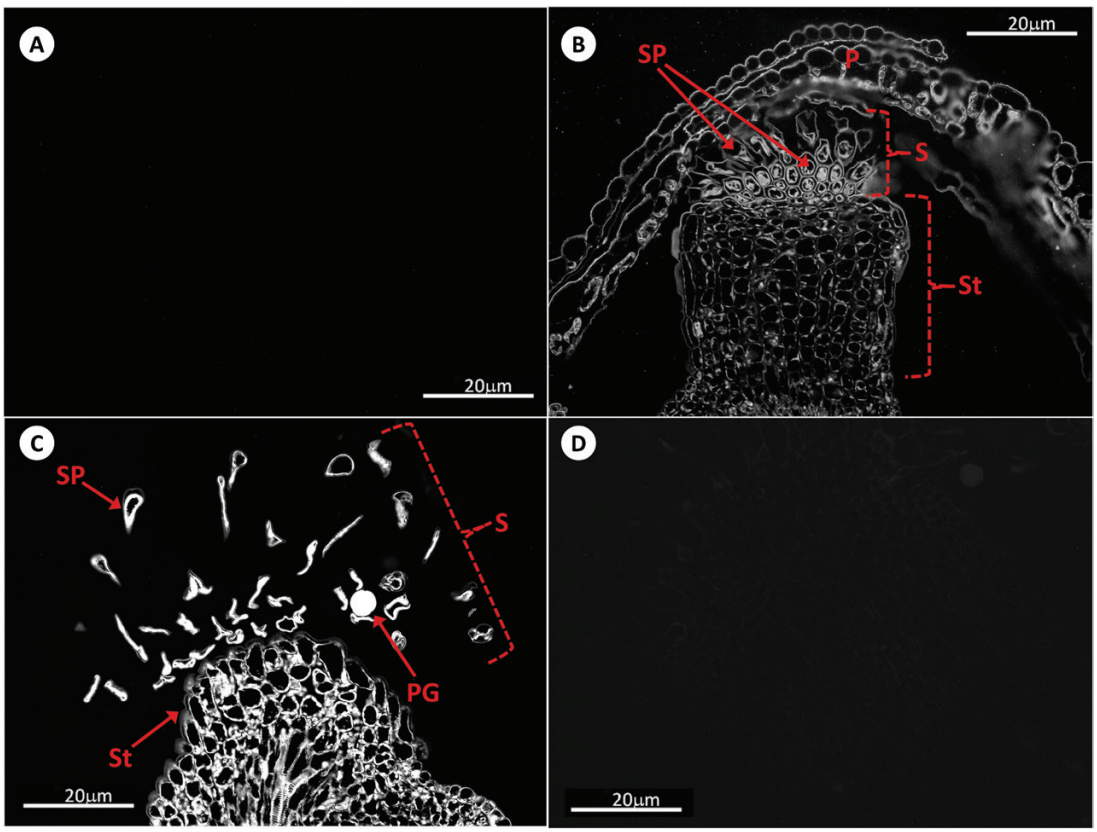

Fig. 6. Immunolocalization of GSH by antibody-associated fluorescence microscopy in Arabidopsis pistils at stage 14. (A) Negative control; (B) WT; (C) roGFP2; (D) *cad2*-1/roGFP2. P, petal; PG, pollen grain; S, stigma; SP, stigmatic papillae; St, style.

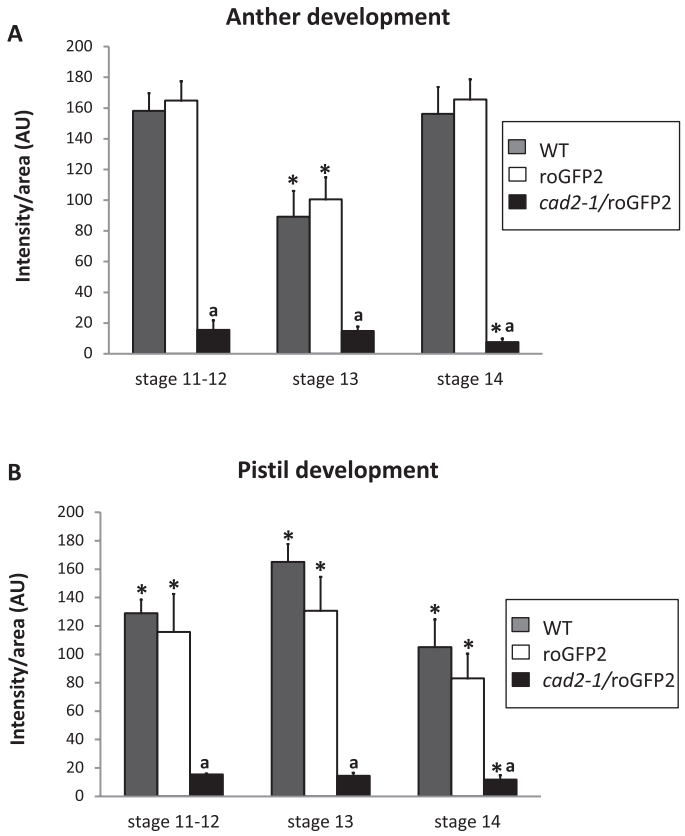

Fig. 7. Relative antibody-associated fluorescence in different organs at different stages of flower development (11–12, 13, and 14) in WT, roGFP2, and *cad2-1*/roGFP2 plants. (A) Development of anthers. (B) Development of pistils. Asterisks indicate statistical significance ($P \leq 0.05$) among the different developmental stages within the same line (roGFP or *cad2-1*). a indicates statistical significance ($P \leq 0.05$) between different lines.

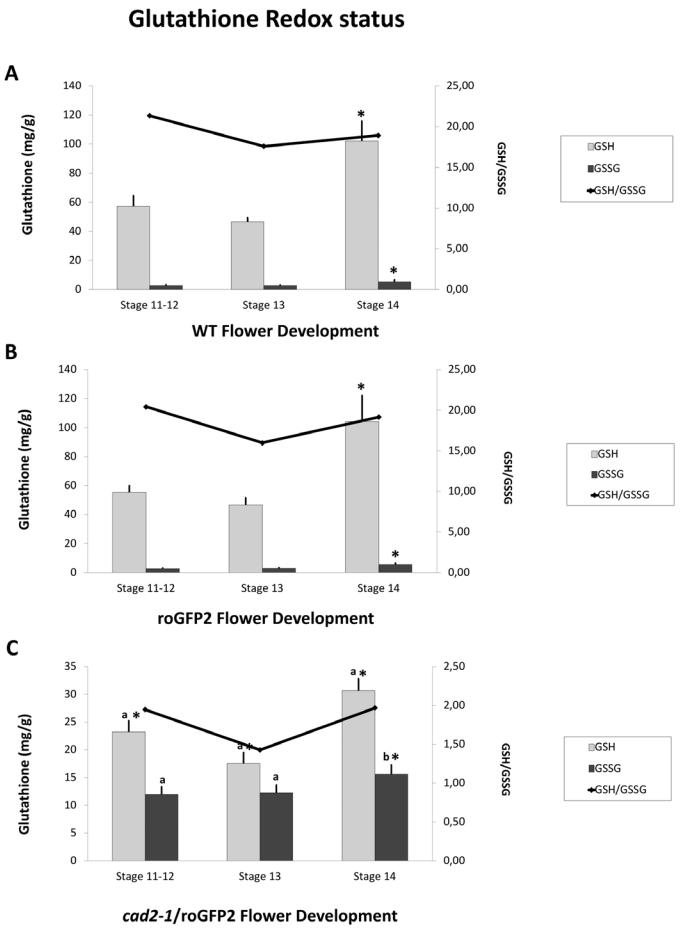

Fig. 8. GSH and GSSG contents and GSH/GSSG ratios of flowers at different stages of development. (A) WT; (B) roGFP2; (C) *cad2-1*/roGFP2. Asterisks indicate statistical significance ($P \leq 0.05$) between different developmental stages. a and b indicate statistical significance at $P \leq 0.01$ and $P \leq 0.05$, respectively, between different lines.

Germination was significantly slower in *cad2-1*/roGFP2 pollen than in roGFP2 pollen (Fig. 14). The germination percentage was also lower in the *cad2-1*/roGFP2 pollen. Pollen tube growth arrested earlier in *cad2-1*/roGFP2 pollen compared with roGFP2 pollen (Fig. 14).Viability experiments demonstrated that the non-germinated pollen grains were alive (data not shown).

Discussion

The redox state of cells is a crucial regulator of metabolism, signalling, and function. While very few tools are available to measure the redox state of living cells, the roGFP probes have proved to be reliable and widely applicable (Meyer *et al.*, 2007; Schwarzländer *et al.*, 2008, 2009; Aller *et al.*, 2013), especially when they incorporate a glutaredoxin (Fernandes *et al.*, 2004; Meyer *et al.*, 2007; Gutscher *et al.*, 2008). The data obtained from roGFP probes therefore provides reliable information concerning the abundance and oxidation state of the glutathione pool *in situ* and *in vivo*. Moreover, roGFP probes have been expressed in a wide variety of cells and organisms, where they can be targeted to specific organelles (Hanson *et al.*, 2004; Birk *et al.*, 2013). The effectiveness of the roGFP2 probes in measuring the redox status of the glutathione pool has previously been demonstrated in studies on other species, such as *Drosophila* (Liu *et al.*, 2012; Aller *et al.*, 2013). The data presented here show that all the tissues of the *cad2-1*/roGFP2 flowers had a lower GSH/GSSG ratio (Fig. 8) and a higher degree of oxidation than the roGFP2 flowers (i.e. in the WT background; Figs 12 and 13). These findings contrast with data from leaves: the level of total glutathione was decreased in the leaves of *cad2-1* mutants but the GSH/GSSG ratios were similar to the WT (Schnaubelt *et al.*, 2015). Taken together, these findings suggest that the flowers of *cad2-1* mutants have a lower capacity to keep the cellular glutathione pool reduced and maintain high GSH/GSSG ratios than the leaves.

A strong association between the extent of glutathione accumulation and flowering time has been demonstrated (Ogawa *et al.*, 2001; Yanagida *et al.* 2004). Flowering was accelerated in the *cad2-1*/roGFP2 mutants compared to the WT (Kocsy *et al.*, 2013). Moreover, glutathione is required for the initiation of the floral meristem (Bashandy *et al.*, 2010, Kocsy *et al.*, 2013) and also pollen tube germination (Zechmann *et al.*, 2011b). The data presented here builds on this firm foundation and reveals the presence of a low degree of oxidation in all the flower parts (stigma, style, anther, germinated pollen grains and pollen tubes) except the ungerminated pollen. Ungerminated pollen exists in a highly oxidized state that is similar to that found in other quiescent cells (Schippers *et al.*, 2016). In contrast to

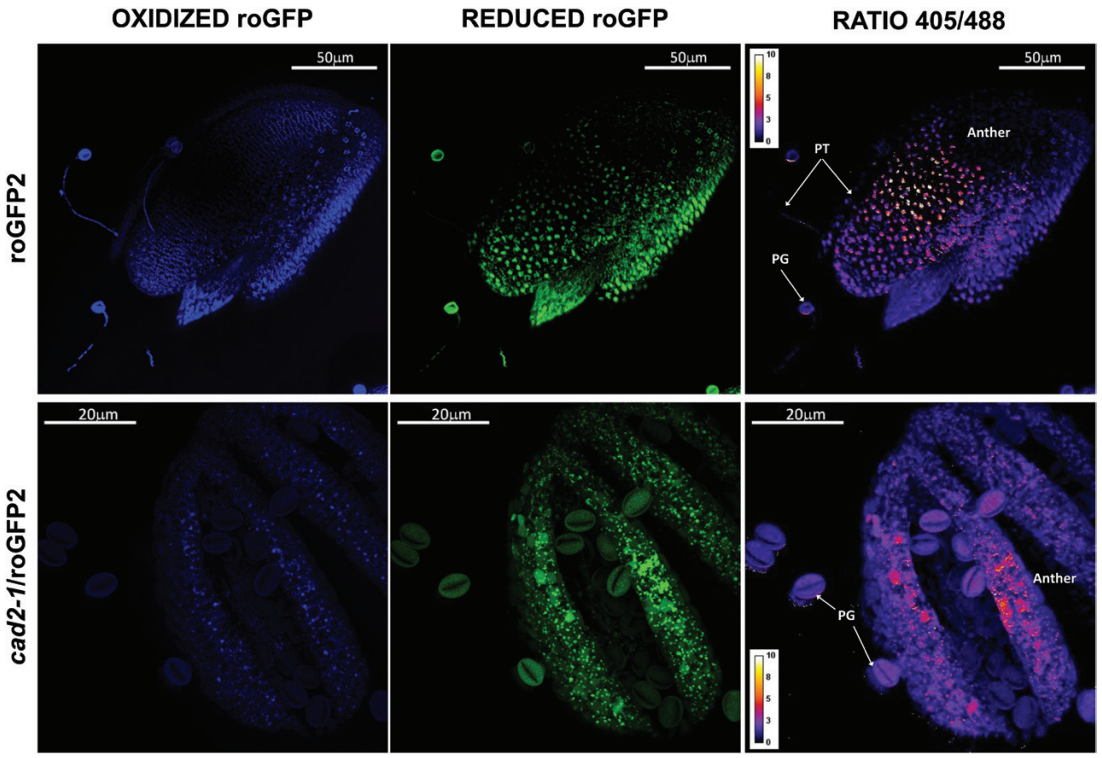

Fig. 9. roGFP fluorescence in anthers with pollen grains at dehiscence (stage 14). The first column shows fluorescence resulting from excitation at 405 nm, the second shows fluorescence resulting from excitation at 488 nm, and the last column shows the ratio of fluorescence at 405/488 nm. PG, pollen grain; PT, pollen tube.

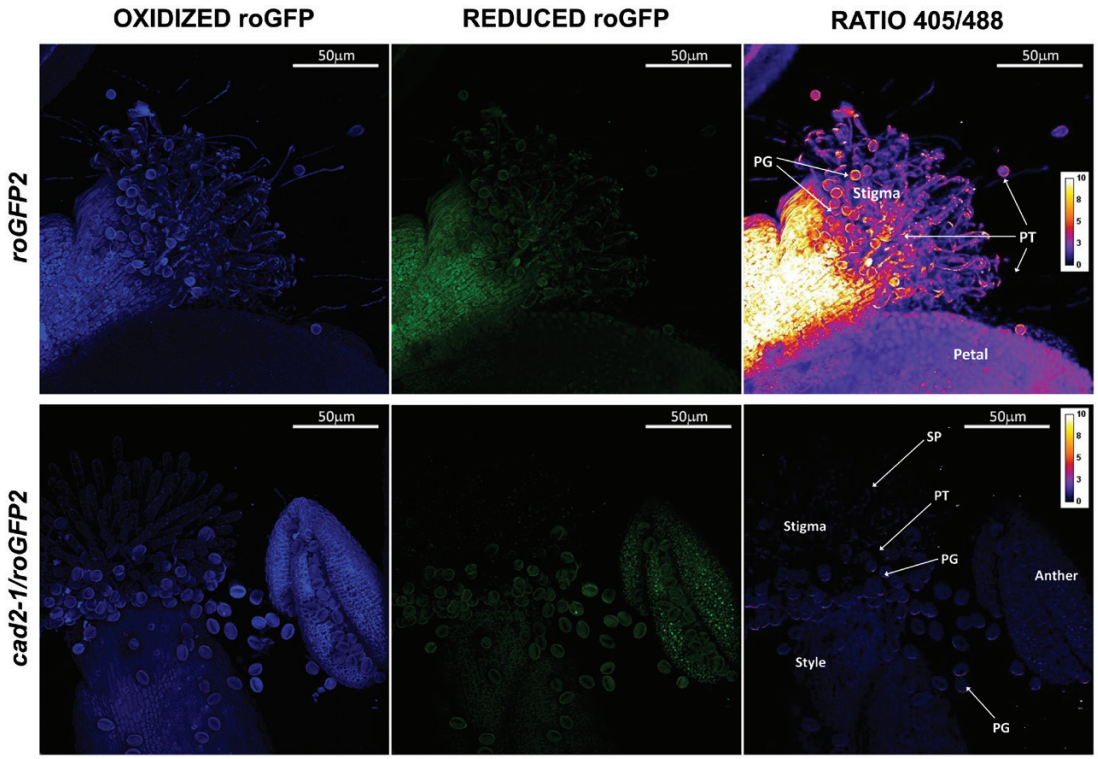

Fig. 10. roGFP fluorescence in flowers (pistil, anther, and germinated pollen) (stage 14) on germination medium. The first column shows fluorescence resulting from excitation at 405 nm, the second shows fluorescence resulting from excitation at 488 nm, and the last column shows the ratio of fluorescence at 405/488 nm. PG, pollen grain; PT, pollen tube; SP, stigmatic papillae.

ungerminated pollen, germinated pollen grains and pollen tubes have a similar degree of oxidation to the other flower parts. These findings suggest that the glutathione pool in pollen is either increased or becomes more reduced (or both) once metabolism is triggered by germination. This process appears to be essential for germination and pollen tube growth because

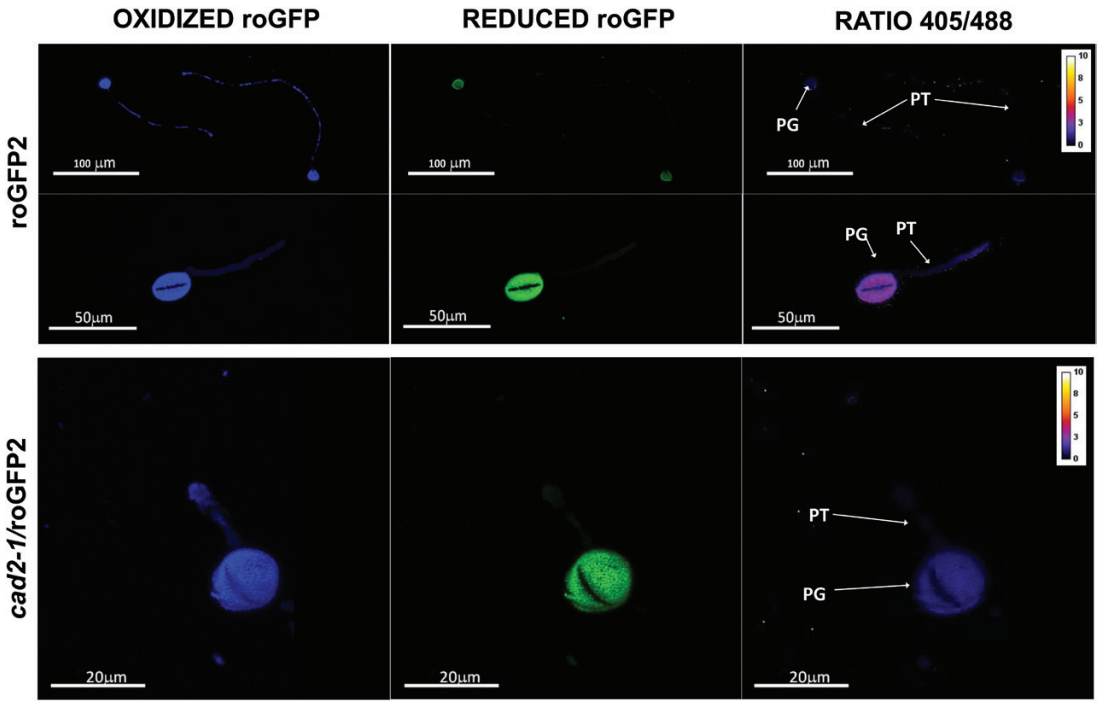

Fig. 11. GFP fluorescence in germinated pollen (stage 14). The first column shows fluorescence resulting from excitation at 405nm, the second shows fluorescence resulting from excitation at 488 nm, and the last column shows the ratio of fluorescence at 405/488 nm. PG, pollen grain; PT, pollen tube.

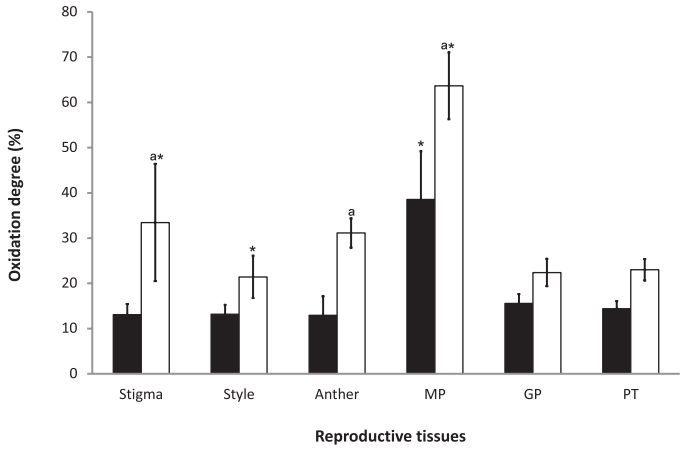

Fig. 12. Degree of oxidation in the stigma, style, anther, ungerminated pollen grains (MP), germinated pollen grains (GP), and pollen tube (PT) in roGFP2 (black bars) and *cad2-1*/roGFP2 (white bars). Asterisks indicate statistical significance ($P \leq 0.05$) among the different tissues within the same line. a indicates statistical significance ($P \leq 0.05$) between the two lines.

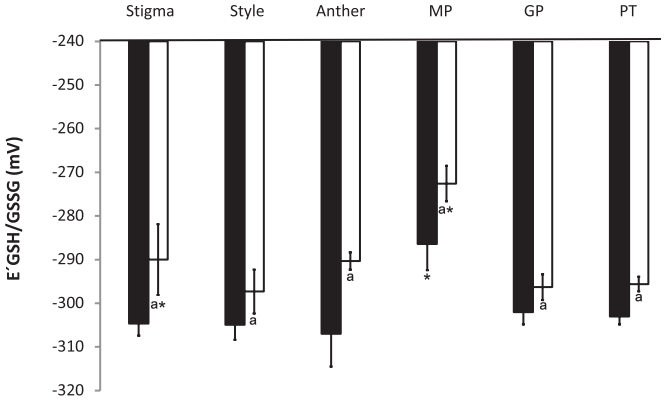

Fig. 13. Redox potential in the stigma, style, anther, ungerminated pollen grains (MP), germinated pollen grains (GP), and pollen tube (PT) in roGFP2 (black bars) and *cad2-1*/roGFP2 (white bars). Asterisks indicate statistical significance ($P \leq 0.05$) among the different tissues within the same line. a indicates statistical significance ($P \leq 0.05$) between the two lines.

these processes are significantly impaired in the *cad2-1*/roGFP2 pollen, which maintained a high degree of oxidation compared with the roGFP2 controls.

The pollen germination rates measured in the WT in the present study were comparable to values in the literature (~71%; Boavida *et al.*, 2007). Germination rates were decreased to ~5–20% in the pollen grains of the *cad2-1*/roGFP2 mutants, which have a restricted capacity for glutathione synthesis (Cobbett *et al.*, 1998; Meyer *et al.*, 2007; Maughan *et al.*, 2010; Zechmann *et al.*, 2011*a, b*; Aller *et al.*, 2013). In addition, the growth rates were much lower in the pollen grains of the mutants. Calculations of glutathione redox potentials based on the roGFP2 measurements confirmed that all the flower parts apart from ungerminated pollen are maintained in a highly reduced state, as is the case for the germinated pollen and pollen tubes. The highly reduced states measured in the germinated pollen show that the endogenous antioxidant systems have sufficient capacity to deal with the large amounts of ROS and reactive nitrogen species produced by the mitochondria (Traverso *et al.*, 2013; Jiménez-Quesada *et al.*, 2016, 2017; Zafra *et al.*, 2018). Interestingly, the mitochondria in leaf cells were found to have the highest concentrations of glutathione of any of the intracellular compartments, even more than the chloroplasts (Zechmann *et al.*, 2008). A roGFP probe targeted specifically to the mitochondria may be useful in future studies of the role of the glutathione pool in pollen tube mitochondria (Rosenwasser *et al.*, 2010).

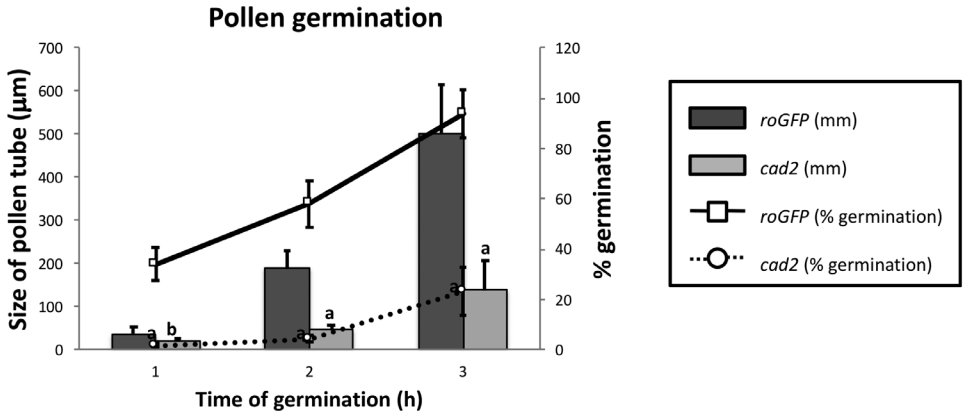

Fig. 14. Differences in *in vitro* pollen germination between freshly opened flowers of roGFP2 and *cad2-1*/roGFP2. The primary axis (on the left and with bars) shows the elongation of the pollen tube during *in vitro* pollen germination. The secondary axis (on the right and with lines) corresponds to the percentage pollen germination measured at the different times of germination. a and b indicate statistical significance at $P \leq 0.01$ and $P \leq 0.05$, respectively.

The finding that the glutathione levels were highest in mature flowers, with a gradual increase in glutathione accumulation during flower development, is interesting. Increasing accumulation ROS during flower development may lead to the oxidative activation of γ-ECS in the plastids, resulting in increased glutathione synthesis and accumulation (Gromes *et al.*, 2008). ROS accumulate during leaf senescence and during the orchestration of programmed cell death because of alterations in the expression of enzymes involved in the antioxidant system and changes in mitochondrial metabolism (Marí *et al.*, 2009; Cui *et al.*, 2012). However, the concept that ROS are pro-life signals generated by aerobic metabolism is widely accepted (Foyer *et al.*, 2018). Open flowers contain mature pollen, which will have already interacted with the pistil to trigger the signalling cascade that results in the germination of the pollen tube. A flow cytometry approach to determine the viability of mature tomato and Arabidopsis pollen related to ROS accumulation revealed that two types of pollen polulations could be identified, namely 'low-ROS' and 'high-ROS' populations, representing low or high metabolic activity, respectively (Luria *et al.*, 2019). The high-ROS pollen germinated with a much higher frequency than the low-ROS pollen (Luria *et al.*, 2019). The metabolically active high-ROS pollen would require high levels of antioxidant activity, particularly high activities of enzymes such as glutathione reductase in order to maintain high GSH/GSSG ratios. Exposure to high temperatures resulted in an increase in the pollen ROS levels and a decrease in germination (Luria *et al.*, 2019). Such stress-induced increases in ROS signals can modify metabolism and cell signalling, particularly if there is no compensating increase in antioxidant capacity. The accumulation of GSSG that was observed in the *cad2-1*/roGFP2 flowers (Figs 8, 12, 13) suggests that the pollen cells were in an oxidized state, which would have a negative impact on pollen–pistil metabolism and pollen tube germination in the mature flowers. Cellular GSSG levels are usually kept at very low levels because this metabolite is not compatible with metabolism. In mutants such as the catalase-deficient *cat2*, where GSSG accumulates, the metabolite is sequestered in the vacuoles (Queval *et al.*, 2011; Noctor *et al.*, 2013). It is therefore likely that much of the GSSG accumulated in the *cad2-1*/roGFP2 flowers is localized in the vacuole and not the cytoplasm. Mature flowers begin to degenerate, undergoing programmed cell death processes, which involve high ROS concentrations (Marí *et al.*, 2009; Ayer *et al.*, 2010). The restriction of glutathione accumulation in the *cad2-1*/roGFP2 flowers and the lower GSH/GSSG ratios may therefore result in faster flower senescence.

Taken together, the data presented here confirm that maintenance of a highly reduced glutathione pool is essential for pollen germination and tube growth (Zechmann *et al.*, 2008). The transition from the oxidized quiescent state to the metabolically active germinated state that facilitates pollen growth therefore requires a large change in cellular redox homeostasis that involves both increased glutathione accumulation and extensive reduction of the glutathione pool. The data presented here show that the capacity to regenerate GSH from GSSG is restricted in *cad2-1*/roGFP2 flowers, as is the ability to synthesize glutathione. These findings demonstrate the importance of cellular redox control in pollen germination and tube growth. Further work is required to demonstrate the nature of the mechanisms involved.

Future studies using combinations of techniques such as roGFP2, fluorochromatic methods (Heslop-Harrison and Heslop-Harrison, 1970), and propidium iodide staining (Jimenez-Quesada *et al.*, 2017) are required to investigate the mechanisms involved in oxidation-induced losses of viability and function. However, current methods that are able to determine the viability of individual pollen grains are difficult to use simultaneously with roGFP2 analysis of redox properties. For example, fluorochromatic detection interferes with the roGFP2 signal because both methods use similar excitation and emission wavelengths.

Pollen grains require a robust antioxidant system to germinate and penetrate through the stigma (Creissen *et al.*, 1999, Zechmann, 2008); further studies are required to determine how much of this defence is constitutive and how much is induced upon alleviation of the quiescent state. The data presented here demonstrate that glutathione is an essential component of this antioxidant defence and perhaps also pollen–stigma signalling through thiol-disulfide exchange mechanisms, protein gluathionylation, and *S*-nitrosoglutathione-mediated processes (Corpas *et al.*, 2013; Zafra *et al.*, 2016). Future work using a range of other mutants and oxidative stress markers is required

to elucidate the redox differences between ungerminated and germinated pollen and to provide a more complete picture of the involvement of GSH metabolism in pollen germination.

Acknowledgements

We thank the Scientific Instrumentation Service (Estación Experimental del Zaidín, CSIC, Granada) for assistance in GC-MS analysis. We also thank the Microscopy Service (Estación Experimental del Zaidín, CSIC, Granada) for help during the confocal microscopy. This work was supported by European Regional Development Fund-co-funded projects BFU2016-77243-P, P2011-CVI7487, RTC2016-4824-2, and RTC2017-6654-2. EGQ thanks the Spanish Ministry of Economy and Competitiveness for "Formación del Personal Investigador" program grant funding.

References

Airaki M, Sánchez-Moreno L, Leterrier M, Barroso JB, Palma JM, Corpas FJ. 2011. Detection and quantification of *S*-nitrosoglutathione (GSNO) in pepper (*Capsicum annuum* L.) plant organs by LC-ES/MS. Plant & Cell Physiology **52**, 2006–2015.

Aller I, Rouhier N, Meyer AJ. 2013. Development of roGFP2-derived redox probes for measurement of the glutathione redox potential in the cytosol of severely glutathione-deficient *rml1* seedlings. Frontiers in Plant Science **4**, 506.

Alvarez-Buylla ER, Benítez M, Corvera-Poiré A, *et al*. 2010. Flower development. The Arabidopsis Book **8**, e0127.

Ayer A, Tan SX, Grant CM, Meyer AJ, Dawes IW, Perrone GG. 2010. The critical role of glutathione in maintenance of the mitochondrial genome. Free Radical Biology & Medicine **49**, 1956–1968.

Ball L, Accotto GP, Bechtold U, *et al*. 2004. Evidence for a direct link between glutathione biosynthesis and stress defense gene expression in Arabidopsis. The Plant Cell **16**, 2448–2462.

Bashandy T, Guilleminot J, Vernoux T, Caparros-Ruiz D, Ljung K, Meyer Y, Reichheld JP. 2010. Interplay between the NADP-linked thioredoxin and glutathione systems in *Arabidopsis* auxin signaling. The Plant Cell **22**, 376–391.

Birk J, Meyer M, Aller I, Hansen HG , Odermatt A, Dick TP, Meyer AJ, Appenzeller-Herzog C. 2013. Endoplasmic reticulum: reduced and oxidized glutathione revisited. Journal of Cell Science **126**, 1604–1617.

Boavida LC, McCormick S. 2007. Temperature as a determinant factor for increased and reproducible in vitro pollen germination in *Arabidopsis thaliana*. The Plant Journal **52**, 570–582.

Cairns NG, Pasternak M, Wachter A, Cobbett CS, Meyer AJ. 2006. Maturation of Arabidopsis seeds is dependent on glutathione biosynthesis within the embryo. Plant Physiology **141**, 446–455.

Cobbett CS, May MJ, Howden R, Rolls B. 1998. The glutathione-deficient, cadmium-sensitive mutant, *cad2-1*, of *Arabidopsis thaliana* is deficient in γ-glutamylcysteine synthetase. The Plant Journal **16**, 73–78.

Considine MJ, Foyer CH. 2014. Redox regulation of plant development. Antioxidants & Redox Signaling **21**, 1305–1326.

Corpas FJ, Alché JD, Barroso JB. 2013. Current overview of *S*-nitrosoglutathione (GSNO) in higher plants. Frontiers in Plant Science **4**, 126.

Creissen G, Firmin J, Fryer M, *et al*. 1999. Elevated glutathione biosynthetic capacity in the chloroplasts of transgenic tobacco plants paradoxically causes increased oxidative stress. The Plant Cell **11**, 1277–1292.

Cui H, Kong Y, Zhang H. 2012. Oxidative stress, mitochondrial dysfunction, and aging. Journal of Signal Transduction **2012**, 646354.

de Simone A, Hubbard R, de la Torre NV, Velappan Y, Wilson M, Considine MJ, Soppe WJJ, Foyer CH. 2017. Redox changes during the cell cycle in the embryonic root meristem of *Arabidopsis thaliana*. Antioxidants & Redox Signaling **27**, 1505–1519.

Fan LM, Wang YF, Wang H, Wu WH. 2001. *In vitro Arabidopsis* pollen germination and characterization of the inward potassium currents in *Arabidopsis* pollen grain protoplasts. Journal of Experimental Botany **52**, 1603–1614.

Fernandes AP, Holmgren A. 2004. Glutaredoxins: glutathione-dependent redox enzymes with functions far beyond a simple thioredoxin backup system. Antioxidants & Redox Signaling **6**, 63–74.

Foyer CH, Noctor G. 2005. Oxidant and antioxidant signalling in plants: a re-evaluation of the concept of oxidative stress in a physiological context. Plant, Cell & Environment **28**, 1056–1071.

Foyer CH, Noctor G. 2009. Redox regulation and photosynthetic organisms: signaling, acclimation, and practical implications. Antioxidants & Redox Signaling **11**, 861–905.

Foyer CH, Noctor G. 2011. Ascorbate and glutathione: the heart of the redox hub. Plant Physiology **155**, 2–18.

Foyer CH, Theodoulou FL, Delrot S. 2001. The functions of inter- and intracellular glutathione transport systems in plants. Trends in Plant Science **6**, 486–492.

Foyer CH, Wilson M, Wright M. 2018. Redox regulation of cell proliferation: Bioinformatics and redox proteomics approaches to identify redox-sensitive cell cycle regulators. Free Radical Biology and Medicine **122**, 137–149.

Galant A, Preuss ML, Cameron JC, Jez JM. 2011. Plant glutathione biosynthesis: diversity in biochemical regulation and reaction products. Frontiers in Plant Science **2**, 45.

García-Quirós E, Carmona R, Zafra D, Claros MG, Alché JD. 2017. Identification and *in silico* analysis of glutathione reductase transcripts expressed in Olive (*Olea europaea* L.) pollen and pistil. In: Rojas I, Ortuño F, eds. Bioinformatics and biomedical engineering: 5th International Work-Conference, IWBBIO 2017, Granada, Spain, April 26–28, 2017, Proceedings, Part II. Cham: Springer, 185–195.

Gigolashvili T, Kopriva S. 2014. Transporters in plant sulfur metabolism. Frontiers in Plant Science **5**, 442.

Gromes R, Hothorn M, Lenherr ED, Rybin V, Scheffzek K, Rausch T. 2008. The redox switch of γ-glutamylcysteine ligase via a reversible monomer–dimer transition is a mechanism unique to plants. Plant Journal **54**, 1063–1075.

Gutscher M, Pauleau AL, Marty L, Brach T, Wabnitz GH, Samstag Y, Meyer AJ, Dick TP. 2008. Real-time imaging of the intracellular glutathione redox potential. Nature Methods **5**, 553–559.

Hanson GT, Aggeler R, Oglesbee D, Cannon M, Capaldi RA, Tsien RY, Remington SJ. 2004. Investigating mitochondrial redox potential with redox-sensitive green fluorescent protein indicators. Journal of Biological Chemistry **279**, 13044–13053.

Heslop-Harrison J, Heslop-Harrison Y. 1970. Evaluation of pollen viability by enzymatically induced fluorescence; intracellular hydrolysis of fluorescein diacetate. Stain Technology **45**, 115–120.

Jimenez-Quesada MJ, Carmona R, Lima-Cabello E, Traverso JÁ, Castro AJ, Claros MG, Alché JD. 2017. Generation of nitric oxide by olive (*Olea europaea* L.) pollen during *in vitro* germination and assessment of the *S*-nitroso- and nitro-proteomes by computational predictive methods. Nitric Oxide **68**, 23–37.

Jiménez-Quesada MJ, Traverso JÁ, Alché JD. 2016. NADPH oxidase-dependent superoxide production in plant reproductive tissues. Frontiers in Plant Science **7**, 359.

Kocsy G, Tari I, Vanková R, Zechmann B, Gulyás Z, Poór P, Galiba G. 2013. Redox control of plant growth and development. Plant Science **211**, 77–91.

Li X. 2011. *Arabidopsis* pollen tube germination. Bio-101, e73. doi: 10.21769/BioProtoc.73

Liu Z, Celotto AM, Romero G, Wipf P, Palladino MJ. 2012. Genetically encoded redox sensor identifies the role of ROS in degenerative and mitochondrial disease pathogenesis. Neurobiology of Disease **45**, 362–368.

López-Mirabal HR, Winther JR. 2008. Redox characteristics of the eukaryotic cytosol. Biochimica et Biophysica Acta **1783**, 629–640.

Luria G, Rutley N, Lazar I, Harper JF, Miller G. 2019. Direct analysis of pollen fitness by flow cytometry: implications for pollen response to stress. The Plant Journal **98**, 942–952.

Marí M, Morales A, Colell A, García-Ruiz C, Fernández-Checa JC. 2009. Mitochondrial glutathione, a key survival antioxidant. Antioxidants & Redox Signaling **11**, 2685–2700.

Marty L, Siala W, Schwarzländer M, Fricker MD, Wirtz M, Sweetlove LJ, Meyer Y, Meyer AJ, Reichheld JP, Hell R. 2009. The NADPH-dependent thioredoxin system constitutes a functional backup for cytosolic glutathione reductase in *Arabidopsis*. Proceedings of the National Academy of Sciences, USA **106**, 9109–9114.

Maughan S, Foyer CH. 2006. Engineering and genetic approaches to modulating the glutathione network in plants. Physiologia Plantarum **126**, 382–397.

Maughan SC, Pasternak M, Cairns N, *et al*. 2010. Plant homologs of the *Plasmodium falciparum* chloroquine-resistance transporter, *Pf*CRT, are required for glutathione homeostasis and stress responses. Proceedings of the National Academy of Sciences, USA **107**, 2331–2336.

Meister A, Anderson ME. 1983. Glutathione. Annual Review of Biochemistry **52**, 711–760.

Meyer AJ, Brach T, Marty L, Kreye S, Rouhier N, Jacquot JP, Hell R. 2007. Redox-sensitive GFP in *Arabidopsis thaliana* is a quantitative biosensor for the redox potential of the cellular glutathione redox buffer. The Plant Journal **52**, 973–986.

Mittler R. 2017. ROS are good. Trends in Plant Science **22**, 11–19.

Mittler R, Vanderauwera S, Gollery M, Van Breusegem F. 2004. Reactive oxygen gene network of plants. Trends in Plant Science **9**, 490–498.

Noctor G, Gomez L, Vanacker H, Foyer CH. 2002. Interactions between biosynthesis, compartmentation and transport in the control of glutathione homeostasis and signalling. Journal of Experimental Botany **53**, 1283–1304.

Noctor G, Mhamdi A, Chaouch S, Han Y, Neukermans J, Marquez-Garcia B, Queval G, Foyer CH. 2012. Glutathione in plants: an integrated overview. Plant, Cell & Environment **35**, 454–484.

Noctor G, Mhamdi A, Foyer CH. 2016. Oxidative stress and antioxidative systems: recipes for successful data collection and interpretation. Plant, Cell & Environment **39**, 1140–1160.

Noctor G, Mhamdi A, Queval G, Foyer CH. 2013. Regulating the redox gatekeeper: vacuolar sequestration puts glutathione disulfide in its place. Plant Physiology **163**, 665–671.

Noctor G, Queval G, Mhamdi A, Chaouch S, Foyer CH. 2011. Glutathione. The Arabidopsis Book **9**, e0142.

Ogawa K, Tasaka Y, Mino M, Tanaka Y, Iwabuchi M. 2001. Association of glutathione with flowering in *Arabidopsis thaliana*. Plant & Cell Physiology **42**, 524–530.

Pasternak M, Lim B, Wirtz M, Hell R, Cobbett CS, Meyer AJ. 2008. Restricting glutathione biosynthesis to the cytosol is sufficient for normal plant development. The Plant Journal **53**, 999–1012.

Queval G, Jaillard D, Zechmann B, Noctor G. 2011. Increased intracellular H_2O_2 availability preferentially drives glutathione accumulation in vacuoles and chloroplasts. Plant, Cell & Environment **34**, 21–32.

Queval G, Thominet D, Vanacker H, Miginiac-Maslow M, Gakière B, Noctor G. 2009. H_2O_2-activated up-regulation of glutathione in *Arabidopsis* involves induction of genes encoding enzymes involved in cysteine synthesis in the chloroplast. Molecular Plant **2**, 344–356.

Rosenwasser S, Rot I, Meyer AJ, Feldman L, Jiang K, Friedman H. 2010. A fluorometer-based method for monitoring oxidation of redox-sensitive GFP (roGFP) during development and extended dark stress. Physiologia Plantarum **138**, 493–502.

Schafer FQ, Buettner GR. 2001. Redox environment of the cell as viewed through the redox state of the glutathione disulfide/glutathione couple. Free Radical Biology & Medicine **30**, 1191–1212.

Schippers JH, Foyer CH, van Dongen JT. 2016. Redox regulation in shoot growth, SAM maintenance and flowering. Current Opinion in Plant Biology **29**, 121–128.

Schnaubelt D, Queval G, Dong Y, Diaz-Vivancos P, Makgopa ME, Howell G, De Simone A, Bai J, Hannah MA, Foyer CH. 2015. Low glutathione regulates gene expression and the redox potentials of the nucleus and cytosol in *Arabidopsis thaliana*. Plant, Cell & Environment **38**, 266–279.

Schnaubelt D, Schulz P, Hannah MA, Yocgo RE, Foyer CH. 2013. A phenomics approach to the analysis of the influence of glutathione on leaf area and abiotic stress tolerance in *Arabidopsis thaliana*. Frontiers in Plant Science **4**, 416.

Schwarzländer M, Fricker MD, Müller C, Marty L, Brach T, Novak J, Sweetlove LJ, Hell R, Meyer AJ. 2008. Confocal imaging of glutathione redox potential in living plant cells. Journal of Microscopy **231**, 299–316.

Schwarzländer M, Fricker MD, Sweetlove LJ. 2009. Monitoring the *in vivo* redox state of plant mitochondria: effect of respiratory inhibitors, abiotic stress and assessment of recovery from oxidative challenge. Biochimica et Biophysica Acta **1787**, 468–475.

Sugiyama A, Nishimura J, Mochizuki Y, Inagaki K, Sekiya J. 2004. Homoglutathione synthesis in transgenic tobacco plants expressing soybean homoglutathione synthetase. Plant Biotechnology **21**, 79–83.

Traverso JA, Pulido A, Rodríguez-García MI, Alché JD. 2013. Thiol-based redox regulation in sexual plant reproduction: new insights and perspectives. Frontiers in Plant Science **4**, 465.

Vanacker H, Harbinson J, Ruisch J, Carver TLW, Foyer CH. 1998. Antioxidant defences of the apoplast. Protoplasma **205**, 129–140.

Vernoux T, Wilson RC, Seeley KA, *et al*. 2000. The *ROOT MERISTEMLESS1/CADMIUM SENSITIVE2* gene defines a glutathione-dependent pathway involved in initiation and maintenance of cell division during postembryonic root development. The Plant Cell **12**, 97–110.

Wachter A, Wolf S, Steininger H, Bogs J, Rausch T. 2005. Differential targeting of GSH1 and GSH2 is achieved by multiple transcription initiation: implications for the compartmentation of glutathione biosynthesis in the *Brassicaceae*. The Plant Journal **41**, 15–30.

Yanagida M, Mino M, Iwabuchi M, Ogawa K. 2004. Reduced glutathione is a novel regulator of vernalization-induced bolting in the rosette plant *Eustoma grandiflorum*. Plant & Cell Physiology **45**, 129–137.

Zafra A, Castro AJ, Alché JD. 2018. Identification of novel superoxide dismutase isoenzymes in the olive (*Olea europaea* L.) pollen. BMC Plant Biology **18**, 114.

Zafra A, Rejón JD, Hiscock SJ, Alché Jde D. 2016. Patterns of ROS accumulation in the stigmas of angiosperms and visions into their multifunctionality in plant reproduction. Frontiers in Plant Science **7**, 1112.

Zafra A, Rodríguez-García MI, Alché Jde D. 2010. Cellular localization of ROS and NO in olive reproductive tissues during flower development. BMC Plant Biology **10**, 36.

Zechmann B. 2014. Compartment-specific importance of glutathione during abiotic and biotic stress. Frontiers in Plant Science **5**, 566.

Zechmann B, Koffler BE, Russell SD. 2011b. Glutathione synthesis is essential for pollen germination in vitro. BMC Plant Biology **11**, 54.

Zechmann B, Liou LC, Koffler BE, Horvat L, Tomašić A, Fulgosi H, Zhang Z. 2011a. Subcellular distribution of glutathione and its dynamic changes under oxidative stress in the yeast *Saccharomyces cerevisiae*. FEMS Yeast Research **11**, 631–642.

Zechmann B, Mauch F, Sticher L, Müller M. 2008. Subcellular immunocytochemical analysis detects the highest concentrations of glutathione in mitochondria and not in plastids. Journal of Experimental Botany **59**, 4017–4027.

Zechmann B, Müller M. 2010. Subcellular compartmentation of glutathione in dicotyledonous plants. Protoplasma **246**, 15–24.